Available online at www.sciencedirect.com
SCIENCE DIRECT®
Journal of Computational Physics 212 (2006) 681–702
JOURNAL OF COMPUTATIONAL PHYSICS
www.elsevier.com/locate/jcp

# Analysis of sponge zones for computational fluid mechanics

Daniel J. Bodony

*Center for Turbulence Research, Stanford University, 488 Escondido Mall, Stanford, CA 94305-3035, United States*

Received 1 March 2005; received in revised form 19 July 2005; accepted 21 July 2005
Available online 1 September 2005

**Abstract**

The use of sponge regions, or sponge zones, which add the forcing term $-\sigma(q - q_{\text{ref}})$ to the right-hand-side of the governing equations in computational fluid mechanics as an ad hoc boundary treatment is widespread. They are used to absorb and minimize reflections from computational boundaries and as forcing sponges to introduce prescribed disturbances into a calculation. A less common usage is as a means of extending a calculation from a smaller domain into a larger one, such as in computing the far-field sound generated in a localized region.

By analogy to the penalty method of finite elements, the method is placed on a solid foundation, complete with estimates of convergence. The analysis generalizes the work of Israeli and Orszag [M. Israeli, S.A. Orszag, Approximation of radiation boundary conditions, J. Comp. Phys. 41 (1981) 115–135] and confirms their findings when applied as a special case to one-dimensional wave propagation in an absorbing sponge. It is found that the rate of convergence of the actual solution to the target solution, with an appropriate norm, is inversely proportional to the sponge strength. A detailed analysis for acoustic wave propagation in one-dimension verifies the convergence rate given by the general theory. The exponential point-wise convergence derived by Israeli and Orszag in the high-frequency limit is recovered and found to hold over all frequencies. A weakly nonlinear analysis of the method when applied to Burgers' equation shows similar convergence properties. Three numerical examples are given to confirm the analysis: the acoustic extension of a two-dimensional time-harmonic point source, the acoustic extension of a three-dimensional initial-value problem of a sound pulse, and the introduction of unstable eigenmodes from linear stability theory into a two-dimensional shear layer.


## 1. Introduction

In recent years, there has been an increasing interest in developing predictive methods for aeroacoustic applications. In a purely numerical prediction, the most fundamental way to determine the flow noise of a given configuration is to solve the compressible Navier–Stokes equations in a large computational domain

*E-mail address:* bodony@stanford.edu.

0021-9991/$ - see front matter © 2005 Elsevier Inc. All rights reserved.
doi:10.1016/j.jcp.2005.07.014

with sufficient resolution to capture the temporal and spatial scales of the noise sources and the radiated sound field. In free shear flows, where the sound is generated by turbulence, one must often provide inflow disturbances at the inlet plane to seed instabilities that promote natural transition to turbulence [1–4]. This must be done quietly in the sense that the inflow conditions not generate spurious noise that may overwhelm the physical sound. A particularly efficient technique of inflow seeding uses forcing sponges where, in a small region of the flow, an additional term $-\sigma(x)(q - q_{\text{ref}})$, is added to the governing equations to 'force' the computed solution to $q$ match the precomputed, unsteady reference solution $q_{\text{ref}}$. Generally the parameter $\sigma$, called the sponge strength, is a function only of space and $q_{\text{ref}}$ a function of space and time. At outflow and lateral boundaries, one may take $q_{\text{ref}}$ to be the steady laminar or RANS (Reynolds averaged Navier–Stokes) solution of a corresponding problem or specified by empirical data to, again, drive the near-boundary field to a known solution, making boundary conditions easier to implement and the calculation less sensitive to the boundary conditions [5].

These uses of sponge regions have in common the addition of the term

$$-\sigma(x)(q - q_{\text{ref}})$$

to the governing equations. The specification of the reference solution and the manner in which the term is implemented – as either inflow forcing or outflow absorbing layers – differentiates the cases. It is the properties of such a term, namely the dependence of the rate of convergence of $q$ to $q_{\text{ref}}$ on $\sigma$, that are the focus of the remainder of this paper.

Israeli and Orszag [6] analyzed the use of sponge regions, which they called 'Newton cooling,' in the specific case of one-dimensional acoustic wave propagation using WKB (Wentzel–Kramers–Brillouin) theory. They found exponential point-wise convergence between the target and actual solutions for acoustic wave propagation in one dimension. Also using WKB they found the reflection coefficient to be a non-monotonic function of the sponge strength. This report confirms and generalizes their analysis to the case of arbitrary frequency and to problems in more than one-dimension. In the case of periodic domains with fringe regions, Nordström et al. [7] also found exponential point-wise convergence. Freund [8] analyzed this technique for the one-dimensional wave equation, where $\sigma$ was taken to be a constant in space. Using Fourier transforms, he found that $q \to q_{\text{ref}}$ as $\sigma^{-1}$. This paper extends these results to multi-dimensional problems with spatially varying $\sigma$.

The use of absorbing layers (perfectly matched layers, PMLs) to minimize reflections in wave propagation problems was further developed by Berenger [9] in electromagnetics and extended to fluid mechanics by Hu [10,11] and Hesthaven [12]. Colonius and Ran [13] proposed a super-grid-scale boundary condition based on windowing the governing equations in physical space. Using an approximate form of their model they find superior results compared to PML in an acoustic reflection problem and roughly equivalent performance to the present method in a convecting nonlinear vortex problem. The sponge layer discussed in the present context differs from the PML and super-grid-scale models in two aspects: (i) it is not formulated to ensure perfect transmission with no reflection (in the case of PML) nor requires modeled dynamics (for the super-grid-scale model) and (ii) it does not involve variable/eigenvalue splitting or require extra spatial derivatives be taken. Because of (ii) sponge regions are particularly appealing. A recent, and excellent, review of absorbing layers, sponge regions, and their variants, was given by Colonius [14].

## 2. Analysis of the sponge regions

If the sponge region problem is slightly restated, similarities are apparent between it and that of the solution of incompressible fluids by mixed or finite elements using penalty methods (see [15,16] and references therein). The mathematical foundation of finite element methods can then be used to determine the properties of the method and, most importantly, the rate of convergence estimate.

We begin by stating the original problem of finding the field $u$ produced by a source distribution. Although the present context deals with fluid mechanics, there is no limitation in applying what follows to other physical problems. Moreover, the identification of the field with a particular set of physical variables, such as the primitive variables (density, pressure and velocity), the conservative variables (mass density, momentum density and energy density), etc., is not necessary as one may be readily transformed into any other. So let $\Omega \subset \mathbb{R}^n$ be a bounded open set with boundary $\partial\Omega$. Then for some finite $T > 0$ consider the problem for $m$ variables $u = [u_1, \ldots, u_m]^{\mathrm{T}}$,

$$\begin{cases} \frac{\partial u}{\partial t} + \sum_{i=1}^{n} A^i \frac{\partial u}{\partial x_i} = f & \text{in } \Omega \times (0,T], \\ u(x,0) = g_1(x) & \text{on } \Omega \times \{t=0\}, \\ Bu(x,t) = h_1(x,t) & \text{on } \partial\Omega \times (0,T], \end{cases} \tag{1}$$

where $u \in V$ for some Hilbert space $V, f, g_1 \in L^2(\Omega)$ and $h_1 \in L^2(\partial\Omega)$. The source term $f$ is presumed to be independent of $u$ and have compact support in $\Omega$. The matrices $A^i \in \mathbb{M}^{m\times m}$, $i = 1, \ldots, n$, may be functions of $x \in \Omega$ and $t \in [0,T]$. The precise choice of $V$ is not important for what follows but only the fact that $V$ has an inner product and norm satisfying the respective axioms. Generally, $V$ will be a Sobolev space (see [17, Chapter 5]). The operator $B$ relates the subset of variables, or their derivatives, that may be specified on the boundary with the imposed condition $h_1(x,t)$.

Now consider the extension problem, where in a spatial region $\Gamma \subset \mathbb{R}^n$ with $\Omega \subset \Gamma$ (see Fig. 1) we wish to find the field $v$ subject to the following: (i) in $\Omega$, the field $v$ faithfully represents $u$ and (ii) in $\Gamma\backslash\Omega$, $v$ is described by the appropriate hyperbolic system. If it were possible, the 'preferred' problem would be stated, with $v \in V$, $g_2 \in L^2(\Gamma)$, $h_2 \in L^2(\partial\Gamma)$, as

$$\begin{cases} \frac{\partial v}{\partial t} + \sum_{i=1}^{n} A^i \frac{\partial v}{\partial x_i} = 0 & \text{in } \Gamma \times (0,T], \\ v(x,0) = g_2(x) & \text{on } \Gamma \times \{t=0\}, \\ Bv(x,t) = h_2(x,t) & \text{on } \partial\Gamma \times [0,T], \\ \text{subject to } v \equiv u & \text{in } \Omega \times [0,T]. \end{cases} \tag{2}$$

The total specification of $v$ in the region $\Omega$ is not valid and an alternative condition in $\Omega$ must be imposed. If, instead of requiring strict equality between $v$ and $u$ in $\Omega$, we want to minimize $\|v-u\|_V$, where $\|\cdot\|_V$ is a norm on elements in the space $V$, then we are led to the problem analogous to penalty methods [15], which may be written

$$\begin{cases} \frac{\partial v}{\partial t} + \sum_{i=1}^{n} A^i \frac{\partial v}{\partial x_i} = -\sigma(v-u) & \text{in } \Gamma \times (0,T], \\ v(x,0) = g_2(x) & \text{on } \Gamma \times \{t=0\}, \\ Bv(x,t) = h_2(x,t) & \text{on } \partial\Gamma \times [0,T], \end{cases} \tag{3}$$

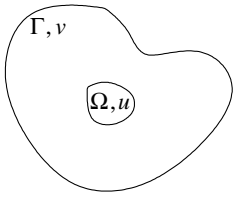


Fig. 1. Schematic of the original domain $\Omega$ with field $u$ and the extended domain $\Gamma$ with field $v$.

where now $\sigma \in \mathbb{M}^{m\times m}$ is a diagonal matrix of strictly positive penalty parameters. The problem originally posed by Freund [8] may be recast as a special case of (3). With the extension problem posed, it is desired to find how the difference $\|v-u\|_V$ depends on $\sigma$. We assume that $\sigma \equiv 0$ outside of $\Omega$.

Determining the convergence properties of $v$ to $u$ as a function of $\sigma$ is straightforward if the weak, or variational, form of (3) is considered. Let $w \in V$ be any suitably smooth test function. Multiply (3) by $w$ and integrate over $\Gamma$. Do similarly for the original system (1) and subtract (1) from (3). With $u$ known in principle in $\Gamma$ (so that the integrals are defined) and having the same boundary conditions on $\partial\Gamma$ as $v$, we find that

$$((v-u)_t, w)_V + \left(\sum_{i=1}^{n} A^i (v-u)_{x_i}, w\right)_V + (\sigma(v-u), w)_V + \langle f, w\rangle - \langle g_2 - g_1, w\rangle = 0, \tag{4}$$

where $(\cdot\,,\cdot)_V$ is an inner product on $V$, $\langle\cdot\,,\cdot\rangle$ denotes the volume integral over $\Gamma$ and $(\cdot)_{x_i} \equiv \partial(\cdot)/\partial x_i$. The second inner product on the left-hand side of (4) may be written as a bilinear form

$$a(v-u, w) = \left(\sum_{i=1}^{n} A^i (v-u)_{x_i}, w\right)_V$$

and similarly for the third term on the left-hand side,

$$b(v-u, w) = (\sigma(v-u), w)_V.$$

The last task is to find a suitable estimate of (4) that demonstrates the convergence properties.

We proceed by re-writing (4) as

$$b(v-u, w) = -((v-u)_t, w)_V - a(v-u, w) - \langle f, w\rangle + \langle g_2 - g_1, w\rangle. \tag{5}$$

Using estimate (1.27) in Chapter II of Brezzi and Fortin [18], we find that

$$\|\sigma\|_{\mathbb{M}^{m\times m}} \|v-u\|_V \leqslant \sup_{w\in V} \left\{ \frac{-((v-u)_t, w)_V - a(v-u, w)}{\|w\|_V} - \frac{\langle f, w\rangle - \langle g_2 - g_1, w\rangle}{\|w\|_V} \right\} \tag{6}$$

or, on using the triangle inequality,

$$\|\sigma\|_{\mathbb{M}^{m\times m}} \|v-u\|_V \leqslant \sup_{w\in V} \frac{((v-u)_t, w)_V}{\|w\|_V} + \|a\| \cdot \|v-u\|_V + \|f\|_{L^2(\Gamma)} + \|g_2 - g_1\|_{L^2(\Gamma)}. \tag{7}$$

If we assume that the matrices $A^i \in C^2(\Gamma \times [0,T]; \mathbb{M}^{m\times m})$, $i = 1, \ldots, n$ (cf. [17]), for $C^2$ being the space of twice continuously differential functions, then $\|a\|$ is finite and continuous with respect to the elements of the $A^i$.

The estimate of $((v-u)_t, w)_V$ needs to be considered in two cases that depend on the initial data, i.e., on specification of $g_2$. For the first case, consider a $g_2$ that is not equal to $u(x,0) = g_1$ so that the initial field of $v$ is not representative of $u$. Then, for $u$ suitably smooth and $\|\sigma\|$ suitably large, the spatial derivatives of $v-u$ will be negligible relative to the right-hand side of the first equation in (3).[1] The reduced equation,

$$(v-u)_t = -\sigma(v-u) \tag{8}$$

has solutions that decay exponentially with time scale $\mathscr{T}$, say. So, for $0 < t < \mathscr{T}$, the time derivative of $v-u$ scales like $\|\sigma\|$ and dominates the remaining terms in estimate (7). For $t > \mathscr{T}$, the right-hand side $-\sigma(v-u)$ no longer dominates in (3) so that the bilinear form $a(v-u, w)$ and inner product $(\sigma(v-u), w)_V$

[1] By considering the weak forms of (1) and (3), we do not require $u$ and $v$ to everywhere continuously differentiable. Instead they may be piecewise continuous and almost everywhere differentiable. In practice, both $u$ and $v$ will be at least $C^1$ due to the action of viscosity [15], so that the estimate of $\|a(v-u, w)\| \ll \|\sigma(v-u)\|$ makes sense.

are important. Then $((v-u)_t, w)_V$ can no longer scale with $\|\sigma\|$ so that the estimate of $((v-u)_t, w)_V$ is $M\|v-u\|_V$ for some constant $M$.

In the second case for estimating $((v-u)_t, w)_V$, the argument of the preceding paragraph shows immediately that if $g_2 = u(x,0)$, then

$$\sup_{w\in V} \frac{((v-u)_t, w)_V}{\|w\|_V} \leqslant M\|v-u\|_V. \tag{9}$$

Combining estimate (9) with (7) leads then to the convergence properties of the proposed method; namely, that

$$\|v-u\|_V \leqslant \frac{\|f\|_{L^2(\Gamma)} + \|g_2 - g_1\|_{L^2(\Gamma)}}{\|\sigma\|_{\mathbb{M}^{m\times m}} - \|a\| - M}, \tag{10}$$

where it is understood that the estimate is valid for times $t > \mathscr{T}$ when the initial conditions on $v$ do not match $u$ at $t = 0$. The most important result of (10) is that $\|v-u\|_V \to 0$ like $\|\sigma\|^{-1}_{\mathbb{M}^{m\times m}}$.

In the analysis just presented, we have assumed that both fields are governed by identical linear hyperbolic equations; some additional elaboration is needed on this point. In practice, the dynamics of the original problem may be nonlinear, as would be the case where $u$ would be determined using the compressible Navier–Stokes equations. This naturally leads to the question of the validity of expressing the original problem as (1). For many problems of interest, the sponge region located near the boundary $\partial\Omega$ is generally 'far', in terms of wavelengths, from the region of nonlinearity. If we take $\Omega$ to be 'far enough' away from the nonlinear processes then the nonlinear equations may be sufficiently well approximated by a linearized set of equations, such as the linearized Euler equations, in which case (1) is justified. A weakly nonlinear analysis is presented in Section 3.3 using Burgers' equation.

In those cases where a forcing sponge is being used, such as near the inflow boundary of a turbulent jet, the evolution of the disturbances is approximately linear so long as the disturbance amplitude remains suitably small. Then for the cases of Reynolds numbers of interest, viscous effects are small and the main role of the mean field on which the disturbances are superposed is to convect the disturbances into the domain and to provide a source of energy for the disturbance growth. In this case, writing the problem as (1) is justified. The forcing problem is discussed in more detail in Section 4.3.

## 3. Detailed solutions in one-dimension

To gain further insight into the rather general analysis presented in Section 2, consider the case of the linear Euler equations in one-dimension. In a medium with pressure $p_0$, density $\rho_0$ and speed of sound $c_0$ the perturbation density $\rho$, the perturbation velocity $u$ and the entropy fluctuation $s$ satisfy the system of equations

$$\begin{aligned}
&\frac{\partial \rho}{\partial t} + \frac{\partial u}{\partial x} = -\sigma_1(\rho - \rho_{\text{ref}}),\\
&\frac{\partial u}{\partial t} + \frac{\partial p}{\partial x} = -\sigma_2(u - u_{\text{ref}}),\\
&\frac{\partial s}{\partial t} = -\sigma_5(s - s_{\text{ref}}).
\end{aligned} \tag{11}$$

Here the density is normalized by $\rho_0$, the velocity by $c_0$, and the pressure by $\rho_0 c_0^2$. The entropy fluctuations are written as $s = (s^* - s^\dagger)/c_v$, where $s^*$ is the dimensional entropy, $s^\dagger$ is a reference entropy state and $c_v$ is the coefficient of specific heat taken at constant volume. The pressure fluctuations $p$ are related to $\rho$ and $s$ via the linearized equation of state

$$p = \rho + \gamma^{-1} s, \tag{12}$$

with $\gamma$ being the ratio of specific heats. Our aim is to determine the functional dependence of $\{\rho, u, s\}$ on the $\{\sigma_i\}$ and the reference states.

For the linear system (11), where the base medium properties and the sponge strengths are independent of time the time-Fourier transform may be used. With the definition of

$$\hat{f}(x;\omega) = \int_{\mathbb{R}} f(t,x) \mathrm{e}^{-\mathrm{i}\omega t}\, \mathrm{d}t \tag{13}$$

we have, from (11), $\{\hat{\rho}, \hat{u}, \hat{s}\}$ as

$$\begin{aligned} \mathrm{i}\omega\hat{\rho} + \frac{\mathrm{d}\hat{u}}{\mathrm{d}x} &= -\sigma_1(\hat{\rho} - \hat{\rho}_{\mathrm{ref}}), \\ \mathrm{i}\omega\hat{u} + \frac{\mathrm{d}\hat{p}}{\mathrm{d}x} &= -\sigma_2(\hat{u} - \hat{u}_{\mathrm{ref}}), \\ \mathrm{i}\omega\hat{s} &= -\sigma_5(\hat{s} - \hat{s}_{\mathrm{ref}}). \end{aligned} \tag{14}$$

Immediately the entropy fluctuations are seen to be one-way coupled to the density and velocity fluctuations so that one may write the result

$$\hat{s} = \frac{\sigma_5}{\sigma_5 + \mathrm{i}\omega} \hat{s}_{\mathrm{ref}} \tag{15}$$

independent of $\hat{\rho}$ and $\hat{u}$.

On using the equation of state (12) and (15), the density and velocity Fourier coefficients satisfy the pair of equations

$$\begin{aligned} (\mathrm{i}\omega + \sigma_1)\hat{\rho} + \frac{\mathrm{d}\hat{u}}{\mathrm{d}x} &= \sigma_1 \hat{\rho}_{\mathrm{ref}}, \\ (\mathrm{i}\omega + \sigma_2)\hat{u} + \frac{\mathrm{d}\hat{\rho}}{\mathrm{d}x} &= \sigma_2 \hat{u}_{\mathrm{ref}} - \frac{1}{\gamma}\frac{\mathrm{d}}{\mathrm{d}x}\left(\frac{\sigma_5}{\sigma_5 + \mathrm{i}\omega}\hat{s}_{\mathrm{ref}}\right). \end{aligned} \tag{16}$$

Eq. (16) may be written as the matrix form of

$$B\hat{q} + A\frac{\mathrm{d}\hat{q}}{\mathrm{d}x} = S \tag{17}$$

with the operators

$$B = \begin{bmatrix} \mathrm{i}\omega + \sigma_1 & 0 \\ 0 & \mathrm{i}\omega + \sigma_2 \end{bmatrix}, \quad A = \begin{bmatrix} 0 & 1 \\ 1 & 0 \end{bmatrix}, \quad S = \begin{bmatrix} \sigma_1 \hat{\rho}_{\mathrm{ref}} \\ \sigma_2 \hat{u}_{\mathrm{ref}} - \frac{1}{\gamma}\frac{\mathrm{d}}{\mathrm{d}x}\left(\frac{\sigma_5}{\sigma_5 + \mathrm{i}\omega}\hat{s}_{\mathrm{ref}}\right) \end{bmatrix}. \tag{18}$$

The general solution to (17) on the open domain $x \in [x_0, +\infty)$ is given by [19] as

$$\hat{q}(x) = \Phi(x - x_0)\xi + \Phi(x)\int_{x_0}^{x} \Phi^{-1}(y) S(y)\, \mathrm{d}y, \tag{19}$$

where $\hat{q}(x_0) = \xi$ is the boundary condition at $x_0$. The fundamental matrix $\Phi(x)$ is the solution to the matrix equation

$$\frac{\mathrm{d}\Phi}{\mathrm{d}x} = -A^{-1}B\Phi, \quad \Phi(x_0) = I \tag{20}$$

with $I$ being the identity matrix. Based on Section 2, we expect that the general behavior of $\hat{q}$ in the sponge region is roughly independent of the details of the problem. Thus we here to consider the simple case of $\sigma_i \equiv$ constant for $i = 1, 2$ and 5, which is equivalent to considering only the problem *in* the sponge region.

One can, for the case of a discontinuous (at $x = x_d$, say) matrix sponge strength $\sigma = \mathrm{diag}(\sigma_1, \sigma_2, \sigma_5)$, formulate the two-zone problem in $x < x_d$ and $x > x_d$ with jump conditions at $x_d$. In this case, the analysis to follow is appropriate for the solution in $x < x_d$. Similar comments apply to the case of smooth $\sigma$. For spatially varying $\sigma$, see the analysis of 3.2.

### 3.1. Solutions with constant sponge strength

For constant matrices $A$ and $B$ from (17), the fundamental solution $\Phi$ is given by the matrix exponential

$$\Phi = \mathrm{e}^{-A^{-1}Bx} = \begin{bmatrix} \cosh(zx) & \frac{a}{z}\sinh(zx) \\ \frac{b}{z}\sinh(zx) & \cosh(zx) \end{bmatrix}, \tag{21}$$

where

$$a = -(\mathrm{i}\omega + \sigma_2), \quad b = -(\mathrm{i}\omega + \sigma_1) \quad \text{and} \quad z^2 = ab. \tag{22}$$

For the square root implied by $z^2 = ab$, the principle branch is suitable. Carrying out the matrix multiplication and taking $\xi = 0$, i.e., only the forced problem, we have

$$\hat{q}(x) = \int_{x_0}^{x} \begin{bmatrix} s_1(y)\cosh[z(x-y)] + \frac{a}{z}s_2(y)\sinh[z(x-y)] \\ \frac{b}{z}s_1(y)\sinh[z(x-y)] + s_2(y)\cosh[z(x-y)] \end{bmatrix} \mathrm{d}y, \tag{23}$$

where $S = [s_1\ s_2]^{\mathrm{T}}$ has been used. An interesting feature of (23) is that the hyperbolic sines and cosines imply that the solution may have exponentially growing behavior, in contrast to the algebraic result of Section 2, unless cancellations occur.

The reference solutions $\hat{\rho}_{\mathrm{ref}}$ and $\hat{u}_{\mathrm{ref}}$ are presumed to be solutions of the homogeneous form of (14) (i.e., with $\sigma \equiv 0$) in which case for $\hat{u}_{\mathrm{ref}}$ one may write

$$\hat{u}_{\mathrm{ref}} = \frac{1}{\mathrm{i}\omega}\left(-\frac{\mathrm{d}\hat{\rho}_{\mathrm{ref}}}{\mathrm{d}x} - \frac{1}{\gamma}\frac{\mathrm{d}\hat{s}_{\mathrm{ref}}}{\mathrm{d}x}\right). \tag{24}$$

Whether the reference solution is steady (i.e., absorbing) or unsteady (forcing) depends on the value of $\omega$: $q_{\mathrm{ref}}$ is steady for $\omega = 0$ and unsteady otherwise. The two cases will be treated separately.

#### 3.1.1. Case 1: Forcing $q_{ref}$ with $\omega \neq 0$

When the reference solution is unsteady corresponds, generally, to the case when one is interested in driving, or forcing, a particular solution. A typical example is the forcing of unsteadiness in a turbulent flow [4]. For an unsteady forcing, we consider the case when $\hat{s}_{\mathrm{ref}} \equiv 0$, which corresponds to forcing with an acoustic reference solution. No unsteady, non-isentropic solutions to the homogeneous form of (14) exist that satisfy $\mathrm{i}\omega\hat{s}_{\mathrm{ref}} = 0$ so that the density and velocity Fourier coefficients satisfy the simple relationship

$$\hat{u}_{\mathrm{ref}} = -\frac{1}{\mathrm{i}\omega}\frac{\mathrm{d}\hat{\rho}_{\mathrm{ref}}}{\mathrm{d}x}, \tag{25}$$

which follows directly from (14). Thus we may write

$$s_2(y) = G\frac{\mathrm{d}s_1(y)}{\mathrm{d}y} \quad \text{with } G = -\frac{1}{\mathrm{i}\omega}\frac{\sigma_2}{\sigma_1}. \tag{26}$$

On substituting (26) into (23) and integrating by parts, we get

$$\hat{q}(x) = \int_{x_0}^{x} \begin{bmatrix} \left(1 + \frac{Gz^2}{b}\right)s_1(y)\cosh[z(x-y)] \\ \left(\frac{z}{a} + Gz\right)s_1(y)\sinh[z(x-y)] \end{bmatrix} \mathrm{d}y + \begin{bmatrix} \frac{Gz}{b}\sinh[z(x-y)]s_1(y) \\ Gs_1(y)\cosh[z(x-y)] \end{bmatrix}_{x_0}^{x}. \tag{27}$$

By a translation of $x$, we can take $x_0 = 0$ for simplicity.

In choosing the form of the reference solution, and hence that of $s_1(y)$, we are free to use a Fourier expansion in $x$ for $\hat{\rho}_{\text{ref}}$. Thus, for an acoustic reference solution we have

$$\hat{\rho}_{\text{ref}}(x) = \tilde{\rho}_{\text{ref}} e^{-ikx}, \tag{28}$$

where $\omega^2 = k^2$ is the acoustic dispersion relation. (Recall the speed of sound has been normalized to unity.) The Fourier amplitude $\tilde{\rho}_{\text{ref}}$ is constant. To force acoustic waves *into* the domain, we take $k > 0$ for $\omega > 0$. Substituting (28) into (27) and carrying out the integration results in the final solution of $\hat{q}(x)$ of

$$\hat{q}(x) = A\sinh(zx) + B\cosh(zx) + Ce^{-ikx}, \tag{29}$$

where

$$A = \begin{bmatrix} \alpha_1\beta \\ \alpha_2\beta^{-1} \end{bmatrix}, \quad B = \begin{bmatrix} -\alpha_2 \\ -\alpha_1 \end{bmatrix} \quad \text{and} \quad C = \begin{bmatrix} \alpha_2 \\ \alpha_1 \end{bmatrix} \tag{30}$$

and

$$\alpha_1 = \frac{\sigma_1^2 + i\omega(\sigma_1+\sigma_2)}{\sigma_1\sigma_2 + i\omega(\sigma_1+\sigma_2)}, \quad \alpha_2 = \frac{\sigma_2^2 + i\omega(\sigma_1+\sigma_2)}{\sigma_1\sigma_2 + i\omega(\sigma_1+\sigma_2)} \quad \text{and} \quad \beta = \left(\frac{i\omega+\sigma_2}{i\omega+\sigma_1}\right)^{1/2}. \tag{31}$$

The forced solution $\hat{q}$ is seen to be the summation of two parts: (i) an exponentially growing/decaying 7portion and (ii) an oscillatory portion. The success of a sponge treatment in forcing a particular reference solution is dependent on the proper selection of the sponge strengths $\sigma_1$ and $\sigma_2$. Only in those cases where $A = -B$, so that the exponentially growing terms of $\sinh(zx)$ and $\cosh(zx)$ cancel, will the application be stable. Thus it is required that

$$\alpha_1\beta = \alpha_2, \tag{32}$$

whose only solution for $\sigma_1, \sigma_2 > 0$ is $\sigma_1 = \sigma_2$. Here, it is seen that only permissible choice is for *equal* sponge strengths, a result that was implicit in [8]. With $\sigma_1 = \sigma_2 := \sigma$ the constant vectors $A$, $B$ and $C$ take the simple form of

$$A, B, C = \begin{bmatrix} 1 \\ 1 \end{bmatrix} \quad \text{for } \sigma_1 = \sigma_2. \tag{33}$$

As a function of $x > x_0$, then we find that point-wise the reference solution $\hat{q}_{\text{ref}}$ and the forced (or desired) solution $\hat{q}$ differ according to

$$\hat{q} - \hat{q}_{\text{ref}} = -2e^{-zx}, \tag{34}$$

which decays exponentially with increasing $x$. In the more general discussion of Section 2, the convergence was based on the norm $\|\cdot\|$ which, for the present case, may be taken as (for a sponge region of length $L$)

$$\|\hat{q} - \hat{q}_{\text{ref}}\| = \int_{x_0}^{x_0+L} \|\hat{q} - \hat{q}_{\text{ref}}\|\, dx \sim \sigma^{-1} \tag{35}$$

in agreement with the analysis of Section 2.

### *3.1.2. Case 2: Absorbing $\hat{q}_{\text{ref}}$ with $\omega = 0$*

In this situation, we are interested in deriving a given solution $\hat{q}$ towards a steady solution $\hat{q}_{\text{ref}}$. The most common usage applies to absorbing boundary treatments [14] that attempt to reduce fluctuation levels of disturbances approaching a computational boundary. Such a boundary treatment has been used by many researchers (see, e.g., [4]).

For this case, we set $\hat{q}_{\text{ref}} = 0$, although the more general reference solution of

$$\hat{u}_{\text{ref}} = \text{constant}, \quad \hat{\rho}_{\text{ref}} = -\frac{1}{\gamma}\hat{s}_{\text{ref}} + \text{constant} \quad \text{and} \quad \hat{s}_{\text{ref}} = f(x), \tag{36}$$

where $f$ is an arbitrary function of $x$, satisfies the homogeneous form of (14). In contrast to the unsteady case where we were interested in the particular solution of (17), it is now the initial value problem in $x$ of the homogeneous system

$$B\hat{q} + A\frac{\mathrm{d}\hat{q}}{\mathrm{d}x} = 0 \tag{37}$$

subject to $\hat{q}(x_0) = \xi$ that is of interest. Again, a translation in $x$ allows us to take $x_0 = 0$ without loss of generality. The solution of (37) was given in (19), which simplifies to

$$\hat{q}(x) = \Phi(x)\xi \tag{38}$$

when $\hat{q}_{\text{ref}} = 0$. With $\Phi$ given by (21) the solution is

$$\hat{q}(x) = \begin{bmatrix} \cosh(zx)\xi_1 + \frac{a}{z}\sinh(zx)\xi_2 \\ \frac{b}{z}\sinh(zx)\xi_1 + \cosh(zx)\xi_2 \end{bmatrix}, \tag{39}$$

where $\xi_1 = \hat{\rho}(0), \xi_2 = \hat{u}(0)$ are the components of $\xi$ at $x = 0$.

Assuming $\hat{\rho}$ and $\hat{u}$ are acoustic solutions that satisfy the homogeneous form of (14), (39) can be expanded as (with $\tilde{u} = k/(\mathrm{i}\omega)\tilde{\rho}$, $\hat{\rho}(x) = \tilde{\rho}\mathrm{e}^{-\mathrm{i}kx}$ and $\hat{u}(x) = \tilde{u}\mathrm{e}^{-\mathrm{i}kx}$)

$$\hat{q}(x) = \begin{bmatrix} \cosh(zx) - \beta\sinh(zx) \\ -\beta^{-1}\sinh(zx) + \cosh(zx) \end{bmatrix}\tilde{\rho}. \tag{40}$$

To ensure a decaying solution one requires that $\sigma_1 = \sigma_2$, similar to the unsteady case. Point-wise $\hat{q}$ approaches $\hat{q}_{\text{ref}} = 0$ exponentially fast with increasing $x$ and the integral error for $x > x_0$ is proportional to $\sigma^{-1}$.

### 3.2. Reflection at a sponge-treated boundary

From the specialized cases with constant sponge strength, it was found that having equal sponge strengths was necessary for stable solutions. It is reasonable to suppose that such a conclusion also follows for those situations with variable sponge strengths. (Although, in practice, the finite sponge zone size limits the overall growth.) Thus we pose the following example that is typical of sponge treatment usage: consider one-dimensional acoustic waves incident on a sponge region of finite length $L$ with sponge strength $\sigma(x)$ (see Fig. 2). We wish to examine the strength of the reflected wave $\hat{q}_s$ due to an incident wave $\hat{q}_i$ and extend the result of Israeli and Orszag [6] to arbitrary frequency.

Because $\sigma$ varies with $x$ we return to the original system (14). In the case of pure acoustic waves, we set $\hat{s} \equiv 0$ so that only the first two equations of (14), for $\hat{\rho}$ and $\hat{u}$, apply. Exploiting the linearity of (14), we may express the problem in an incident wave/scattered wave form by setting

$$\hat{q} = \hat{q}_{\text{i}} + \hat{q}_{\text{s}}, \tag{41}$$

where $\hat{q}_{\text{i}}$ is the incident, right-traveling acoustic wave and $\hat{q}_{\text{s}}$ is the scattered, left-traveling acoustic wave. Away from the sponge, where $\sigma = 0$, $\hat{q}_{\text{i}}$ and $\hat{q}_{\text{s}}$ have simple forms. In the sponge region, we choose to damp the perturbations so that $\hat{q}_{\text{ref}} = 0$. Thus the governing equations for the scattered field are

$$\begin{aligned} (\mathrm{i}\omega + \sigma)\hat{\rho}_{\text{s}} + \frac{\mathrm{d}\hat{u}_{\text{s}}}{\mathrm{d}x} &= -\sigma\hat{\rho}_{\text{i}}, \\ (\mathrm{i}\omega + \sigma)\hat{u}_{\text{s}} + \frac{\mathrm{d}\hat{\rho}_{\text{s}}}{\mathrm{d}x} &= -\sigma\hat{u}_{\text{i}}. \end{aligned} \tag{42}$$

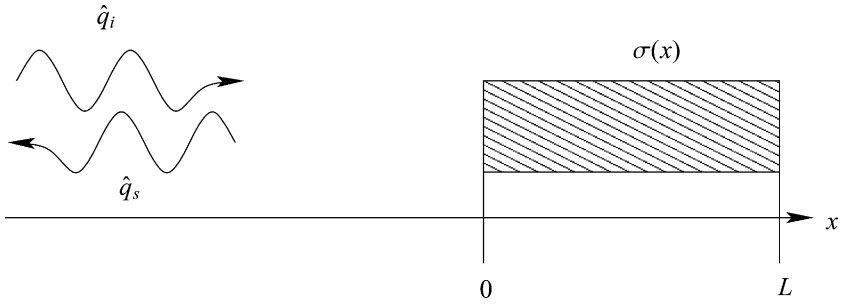


Fig. 2. One-dimensional acoustic waves impinging on a sponge zone.

For an incident field of the form $\hat{q}_\mathrm{i} = \tilde{q}_\mathrm{i} \mathrm{e}^{-\mathrm{i}kx}$, with $k = \omega > 0$, the boundary conditions are as follows. At $x = L$, a solid wall is placed so that $\hat{u} = 0$. As $x \to -\infty$, we expect a left-traveling acoustic wave, of unknown strength, to propagate: $\hat{q}_\mathrm{s} \sim \mathrm{e}^{+\mathrm{i}kx}$ with $k > 0$. Note that the factor $(\mathrm{i}\omega + \sigma)$ in (42) can be written as $\mathrm{i}\omega_\mathrm{eq}$, where $\omega_\mathrm{eq} = \omega - \mathrm{i}\sigma$ is an equivalent complex frequency. In the time-Fourier space, the damping may be interpreted as a complex-valued frequency.

It is expedient, in terms of applying boundary conditions, to solve the problem in the form of a single equation for the scattered velocity $\hat{u}_\mathrm{s}$. Taking the $x$-derivative of the first equation of (42) and using the second equation of (42) yields the second-order equation

$$\frac{\mathrm{d}^2 \hat{u}_\mathrm{s}}{\mathrm{d}x^2} - \frac{1}{\mathrm{i}\omega + \sigma} \frac{\mathrm{d}\sigma}{\mathrm{d}x} \frac{\mathrm{d}\hat{u}_s}{\mathrm{d}x} - \frac{(\mathrm{i}\omega + \sigma)^2}{c_0^2} \hat{u}_\mathrm{s} = -\frac{\mathrm{i}}{\omega} \left( 1 + \frac{\sigma}{\mathrm{i}\omega + \sigma} \right) \frac{\mathrm{d}\sigma}{\mathrm{d}x} \frac{\mathrm{d}\hat{u}_\mathrm{i}}{\mathrm{d}x} - \sigma^2 \hat{u}_\mathrm{i} := \hat{s}(x). \tag{43}$$

The boundary conditions are

$$\begin{aligned} &\hat{u}_\mathrm{s} = -\hat{u}_\mathrm{i} \quad \text{at } x = L, \\ &\hat{u}_\mathrm{s} \sim \mathrm{e}^{+\mathrm{i}kx} \quad \text{at } x \to -\infty, \end{aligned} \tag{44}$$

with $\hat{u}_\mathrm{i} = \tilde{u}_\mathrm{i} \mathrm{e}^{-\mathrm{i}kx}$.

Away from the sponge, where $\sigma = 0$, the limiting form of (43),

$$\frac{\mathrm{d}^2 \hat{u}_\mathrm{s}}{\mathrm{d}x^2} + \omega^2 \hat{u}_\mathrm{s} = 0 \tag{45}$$

has $\mathrm{e}^{\pm \mathrm{i}kx}$ as solutions. Thus for $x < 0$ we expect $\hat{u}_\mathrm{s}$ to be

$$\hat{u}_\mathrm{s} = A \mathrm{e}^{-\mathrm{i}kx} + B \mathrm{e}^{\mathrm{i}kx}, \tag{46}$$

where $A$ and $B$ are complex coefficients. For $x \geqslant 0$, the form of $\hat{u}_\mathrm{s}$ depends on the specific sponge distribution chosen. A commonly used variation is

$$\sigma = \eta (x/L)^n H(x) \tag{47}$$

for non-negative integer $n$. $H(x)$ is the Heaviside function defined as $H(x) = 0$ for $x < 0$ and $H(x) = 1$ for $x > 0$. The sponge strength is controlled by the positive parameter $\eta$. With this form of $\sigma$ the general homogeneous solution of (43) is

$$\hat{u}_\mathrm{sh} = A \mathrm{e}^{-\mathrm{i}kx - H(x)\xi_n} + B \mathrm{e}^{+\mathrm{i}kx + H(x)\xi_n} = A y_1(x) + B y_2(x), \tag{48}$$

where $\xi_n = \eta x^{n+1}/[(n+1)L^n]$. The particular solution of (42) is given by [19]

$$\hat{u}_\mathrm{sp} = -y_1(x) \int^x \frac{y_2(t)\hat{s}(t)}{W(y_1, y_2)} \mathrm{d}t + y_2(x) \int^x \frac{y_1(t)\hat{s}(t)}{W(y_1, y_2)} \mathrm{d}t, \tag{49}$$

with $W(y_1, y_2) = y_1 y_2' - y_2 y_1'$ being the Wronskian and $()'$ denoting differentiation with respect to $x$. The full scattered solution is then the sum of the homogeneous and particular solutions:

$$\hat{u}_s = \hat{u}_{sh} + \hat{u}_{sp}. \tag{50}$$

Application of boundary conditions (44) shows that $A = 0$ for a left traveling wave and $B$ is chosen to satisfy the zero-velocity condition ($\hat{u}_s = -\hat{u}_i$) at $x = L$.

The property of the solution that is most of interest is the reflected wave, $\hat{u}_s$, as $\eta$ increases for fixed $x < 0$. As a function of $n$ we find that, using (48) and (49),

$$\hat{u}_s \sim \begin{cases} \eta & \text{for } n = 0, \\ L\eta e^{-L\eta/(n+1)} & \text{for } n = 1, 2, \ldots, \end{cases} \tag{51}$$

as $\eta, L \to \infty$. When $n = 0$ and the sponge strength is discontinuous, the sponge length does not influence the results to leading order and the reflected wave *increases* in amplitude with increase sponge strength $\eta$. Once, however, the sponge strength is continuous ($n \geqslant 1$) the reflected wave has an exponentially decaying amplitude as the sponge strength and the sponge length are increased. As the polynomial order $n$ of the sponge strength distribution function is increased, the reflected wave amplitude also increases, albeit slightly, for fixed $\eta$. These scalings are verified in Fig. 3. Note that Fig. 3 reproduces Fig. 3 of Israeli and Orszag [6] but is not restricted by the limits necessary for WKB validity.

### 3.3. Weakly nonlinear analysis of Burgers' equation

Thus far the widely applicable linear analysis of Section 2 was verified in the linear problems described above. While a similar theory applicable to nonlinear systems of equations is not available, experience suggests that (nearly) equivalent convergence rates apply in nonlinear problems commonly found in fluid mechanics. To verify this observation in the context of a weakly nonlinear analysis we appeal to the model problem of inviscid Burgers' equation which is the appropriate limiting case in a few problems in aerodynamics [20]. Thus consider Burgers' equation in $\mathbb{R}^n$, for $n = 1, 2, 3$,

$$\frac{\partial q}{\partial t} + [(U + q) \cdot \nabla] q - \nu \frac{\partial^2 q}{\partial x_k \partial x_k} = -\sigma(q - q_{ref}), \tag{52}$$

where $U$ is a constant vector. The Cole–Hopf transformation [20] provides a means to determine analytical solutions of (52), with $\sigma \equiv 0$, when $q = -2\nu\nabla\theta$ and $\theta$ satisfies the heat equation $\partial_t \theta = \nu \nabla^2 \theta$. When $\sigma \neq 0$ the Cole–Hopf transformation does not apply. However, if we take $\nu \equiv 0$ then we may apply the method of characteristics in solving (52).

Suppose that $v$ is a solution to (52) with $\sigma \equiv 0$ and represents the target solution. Then set $q = v + \epsilon w$ with $0 < \epsilon \ll 1$. Substituting, letting $w = w_0 + \epsilon w_1 + \cdots$, and separating by polynomial powers of $\epsilon$ we find that

$$\epsilon^0 : \quad \partial_t w_0 + [(U + v) \cdot \nabla] w_0 = -(\sigma + \nabla v) w_0, \tag{53}$$

$$\epsilon^1 : \quad \partial_t w_1 + [(U + v) \cdot \nabla] w_1 = -(\sigma + \nabla v) w_1 - (w_0 \cdot \nabla) w_0 \tag{54}$$

with similar equations for $\epsilon^p$ for integer $p > 1$. The equation for $w_0$ may be solved by the method of characteristics by defining $s(t, x_0)$ to be the scalar coordinate along the characteristic starting with $s = 0$ at $x = x_0$. Along the characteristic $w_0$ satisfies

$$\frac{dw_0}{ds} + (\sigma + \nabla v) w_0 = 0, \tag{55}$$

$$\frac{dx}{ds} = U + v, \tag{56}$$

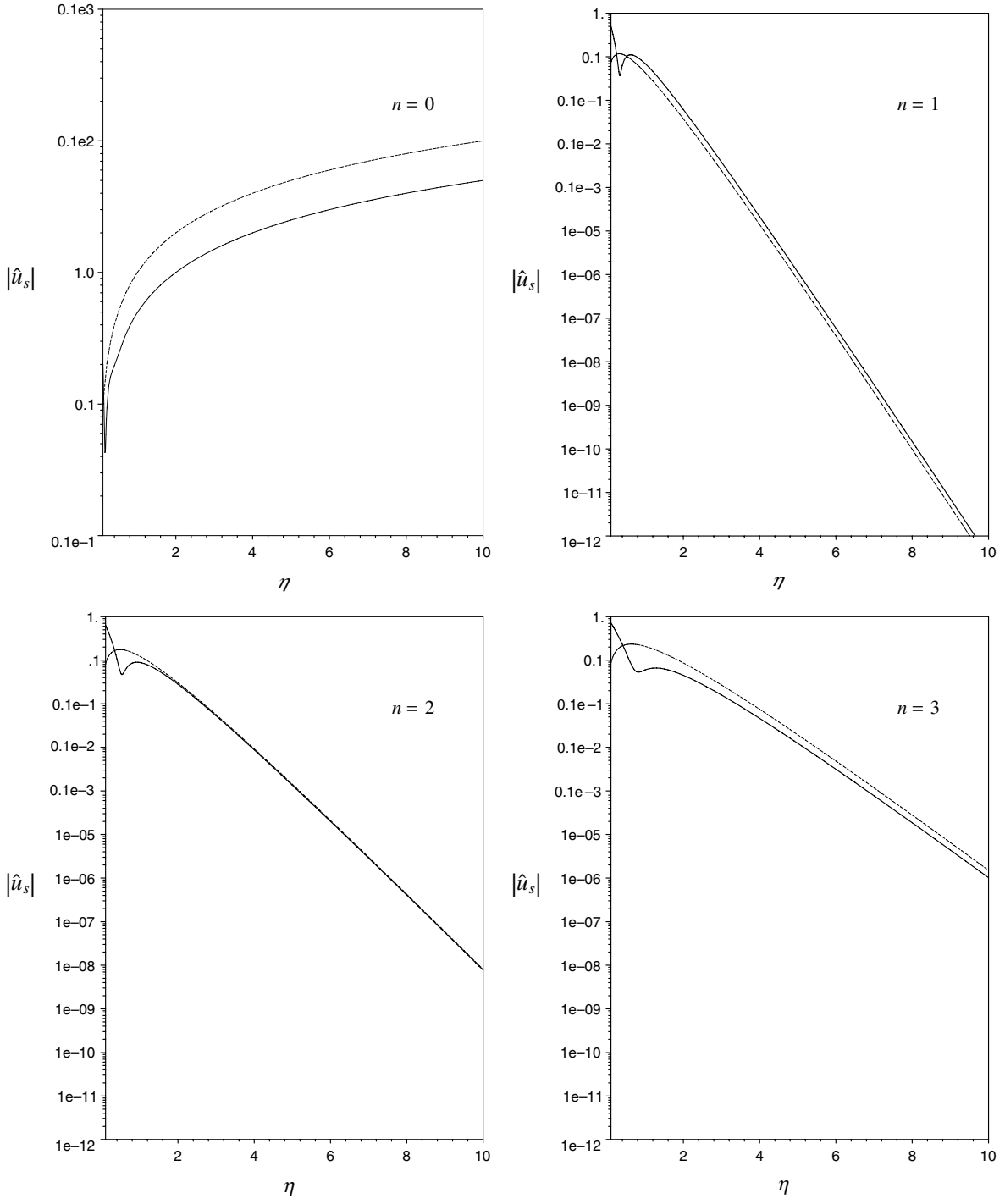


Fig. 3. Reflected wave amplitude (solid) and its asymptotic form (dashed) as a function of sponge strength. The amplitude is measured at $x = -\lambda$, where $\lambda = 2\pi/\omega$ is the acoustic wavelength, for an incident wave of strength $\|\hat{u}_i\| = 1$. The sponge length is taken as $L = \lambda$.

where d/d$s$ is the derivative along the characteristic. We may formally solve the second of these equations as

$$x(x_0, s) = \int_0^s (U + v)(s')\,\mathrm{d}s' + x_0 \tag{57}$$

and the first as

$$w_0(x_0, s) = \Phi(s)\xi, \tag{58}$$

where $\Phi$ satisfies the matrix equation

$$\frac{\mathrm{d}\Phi}{\mathrm{d}s} = -(\sigma + \nabla v)\Phi \quad \text{subject to } \Phi(0) = I \tag{59}$$

and $\xi$ is the value of $w_0$ at $s = 0$.

In the limiting case where $\|\sigma\| \gg \|\nabla v\|$ we have, because $\sigma$ is diagonal, the result that $\Phi(s) \approx \exp[-\int_0^s \sigma(s')\mathrm{d}s']$ so that $w_0$ decays exponentially along the characteristic. A similar conclusion holds when, as $s \to \infty$, $\sigma$ approaches a constant (non-zero) matrix and $\nabla v \to 0$ [19]. When the analysis is carried out to order $\epsilon^1$ one finds that $\|w_0\| \gg \|w_1\|$ as $s \to \infty$ under these conditions.

From this we conclude that for the irrotational, convective flow modeled by Burgers' equation the weakly nonlinear analysis shows an approximately exponential point-wise convergence of $q$ to $q_{\mathrm{ref}}$ *along the characteristic* for those cases where the asymptotic solutions of (59) may be found. It is here emphasized, however, that one should be cautious in extrapolating these results to more general nonlinear systems, especially to those where coupling is important.

## 4. Numerical examples in two and three dimensions

Although the analysis of Section 3 was carried out in one-dimension, the overall convergence estimate in (10) is valid in more general spaces. To illustrate this additional numerical examples are presented for two- and three-dimensional problems.

### 4.1. Two-dimensional harmonic acoustic problem

Consider a two-dimensional space with uniform properties $\rho_0$ and $c_0$. For the problem of linear acoustic propagation in an inviscid medium, the operators $A^i$ of (1) take the particularly simple form of the constant matrices

$$A^1 = \begin{bmatrix} 0 & \rho_0 & 0 & 0 \\ 0 & 0 & 0 & \rho_0^{-1} \\ 0 & 0 & 0 & 0 \\ 0 & \gamma p_0 & 0 & 0 \end{bmatrix}, \qquad A^2 = \begin{bmatrix} 0 & 0 & \rho_0 & 0 \\ 0 & 0 & 0 & 0 \\ 0 & 0 & 0 & \rho_0^{-1} \\ 0 & 0 & \gamma p_0 & 0 \end{bmatrix},$$

when using primitive variables $u = [\rho\ u_x\ u_y\ p]^{\mathrm{T}}$. The problem was first solved using the time-dependent Euler equations linearized about a quiescent medium with the source present. The variables are non-dimensionalized by the ambient density $\rho_0$, the ambient speed of sound $c_0$, and the length $\ell$. The prescribed source distribution is that of a time-harmonic source located in the pressure and density equations of the form

$$f = [1\ 0\ 0\ 1]^{\mathrm{T}} \exp(-4r^2)(\sin(\pi t) + 8\sin(2\pi t)), \quad r^2 = x^2 + y^2.$$

The computation domain is a square with sides of length $20\ell$ with $201 \times 201$ points uniformly spaced in the $x$- and $y$-directions. Poinsot and Lele [21] non-reflecting boundary conditions were implemented on all four sides. Along each edge, with normal coordinate $\zeta$, an absorbing sponge with strength

$$\sigma_{\mathrm{a}} = \left( \frac{\|\zeta\|/\ell - 8}{10 - 8} \right)^3 \tag{60}$$

for $|\zeta|/\ell \geqslant 8$ is placed. The width of sponge region is equal to the longest acoustic wavelength $\lambda = 2\ell$, corresponding to 20 points. Time integration used the fourth-order Runge–Kutta (RK4) algorithm with a time step of $\Delta t = 0.01\ell/c_0$ corresponding to a CFL of approximately 0.5.

Using the present method of (3), the problem was 're-solved' in the same domain with the same boundary conditions but with the knowledge of the original field $u$ limited to circle centered at the origin and of radius slightly greater than two. The form of $\sigma_f$ chosen was

$$\sigma_f = \begin{cases} \sigma_{\max} \exp(-4(r-1)^2) & \text{for } r > 1, \\ \sigma_{\max} & \text{for } r \leqslant 1, \end{cases} \tag{61}$$

where $\sigma_{\max}$ is a parameter. See the sketch in Fig. 4.

Fig. 5 shows the pressure field at a time approximately six periods, based on the lowest frequency, after the simulation was started, along a line running through the origin with $\sigma_{\max} = 100$. Only part of the total domain is shown. In this case, the initial conditions were $v = 0$ so that there was a significant difference in $v - u$ at the start. By the time shown, the initial condition discrepancy does not appear and there is agreement between the two fields. Over three orders of magnitude of $\|\sigma\|$ (see Fig. 6), the convergence follows the $\|\sigma\|^{-1}$ rate.

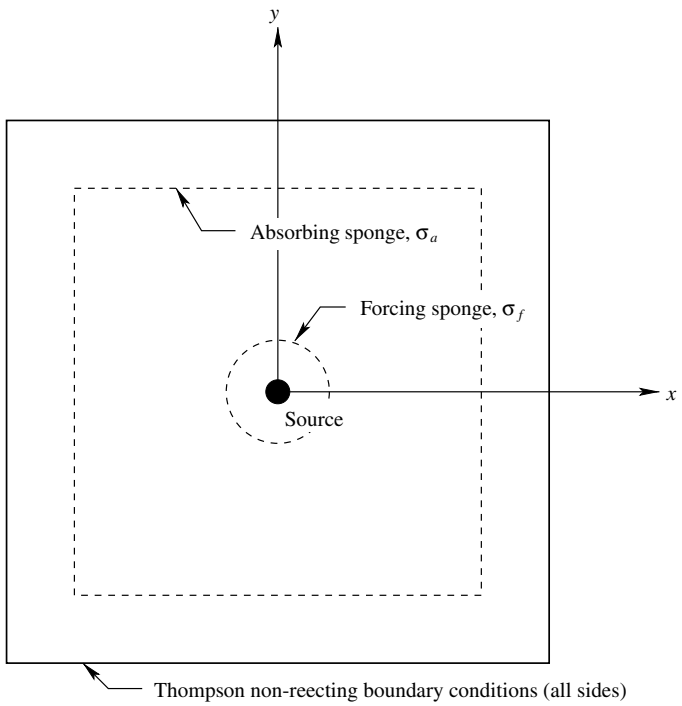


Fig. 4. Schematic of two-dimensional acoustic wave propagation produced by a time-harmonic source.

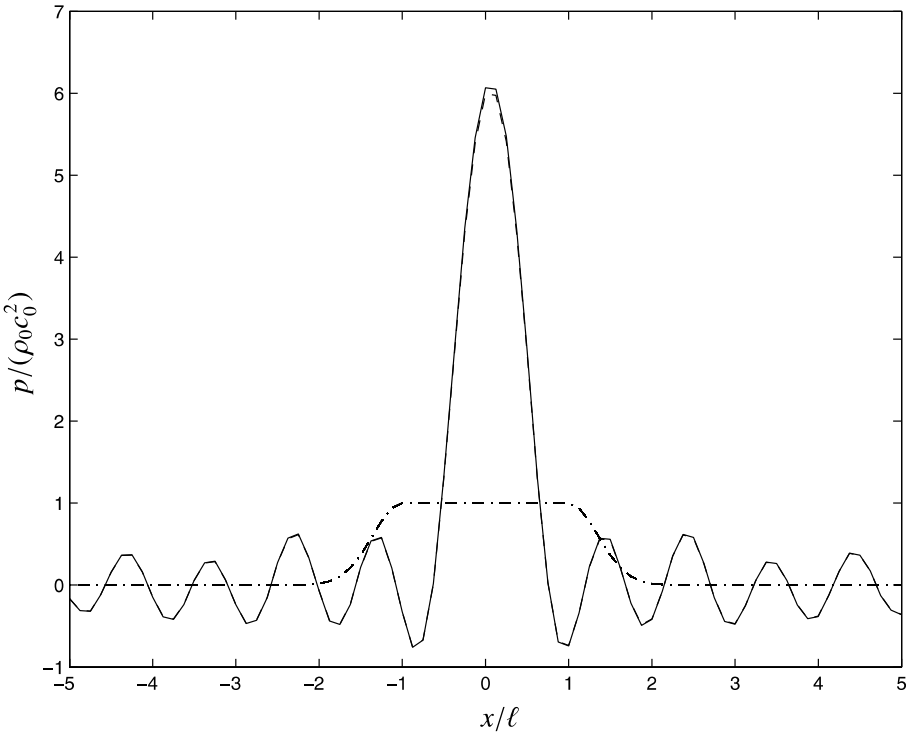


Fig. 5. Pressure field of two, two-dimensional monopoles computed using solution extension method of problem (3). Solid line ——, exact solution; dotted line – – –, numerical solution; dash-dot line –·–, penalty parameter $\sigma(x)/\sigma_{\max}$.

The two-dimensional time harmonic problem does not provide evidence that the proposed penalty method is useful for transient events. Thus a three-dimensional transient problem, that of a Gaussian acoustic pulse centered at the origin, is presented next.

### 4.2. Three-dimensional transient acoustic problem

For the three-dimensional wave equation in free space, the field $u$ is given by

$$\begin{cases} \frac{\partial^2 u}{\partial t^2} - \Delta u = 0, \\ u(x,0) = g(x), \\ \frac{\partial u}{\partial t}(x,0) = h(x). \end{cases} \tag{62}$$

The initial data of the pulse is

$$g(x) = \exp\left(-r^2\right), \quad r^2 = x^2 + y^2 + z^2,$$
$$h(x) = 0.$$

The three-dimensional problem is solved in the same manner as the two-dimensional problem: the domain consists of a cube with sides of length $20\ell$ on a grid of $101 \times 101 \times 101$. The six faces of the cube use the same non-reflecting boundary conditions described previously. $\sigma_{\max}$ was taken to be 100 with spatial distribution $\sigma_f = \sigma_{\max}\exp(-4r^2)$. The pressure field of part of the domain along a line parallel to the $x$-axis and running through the origin is shown in Fig. 7 for three instances of time: $t = 1$, 2 and 3. Agreement between the two fields for all three times is clear and the penalty method is seen to work well for transient problems.

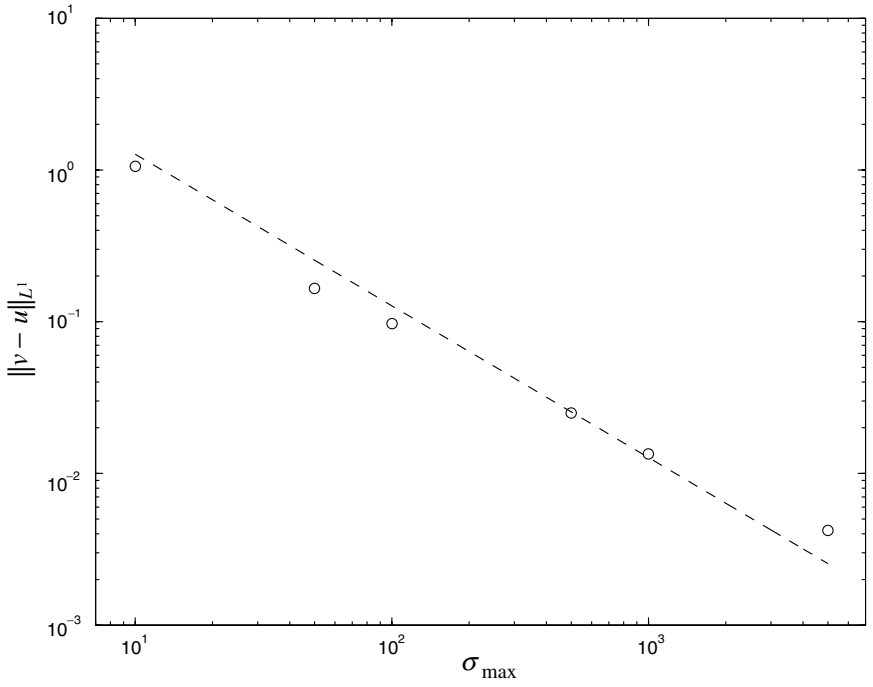


Fig. 6. Convergence of extended problem to original problem for various strengths of the penalty parameter $\sigma$. Dashed line — —, $\sigma_{\max}^{-1}$; open circles ○, numerical results.

### 4.3. Forcing instability waves into a two-dimensional shear layer

In the calculations of Freund [1], Zhao et al. [2] and Bodony and Lele [4], for example, a forcing sponge was used to introduce unsteady disturbances into a free shear flow in a controlled manner. In the latter two studies, homogeneous solutions of an appropriate linearized Euler system (to be described below) were used to introduce the disturbances *without* generating sound at the computational boundary (cf. [22]). While we do not have an analysis appropriate to nonlinear systems of equations analogous to that described in Section 2, we do expect the general conclusions to hold approximately based on the weakly nonlinear analysis Burgers' equation in Section 3.3. This hypothesis is tested on the introduction of instability waves into a two-dimensional shear layer.

The two-dimensional shear layer is shown in Fig. 8. The upper stream is quiescent while the lower stream has a Mach number of 1.2. The static pressure $p_\infty$ is constant across the layer while both streams have the same temperature $T_\infty$ as $|y| \to \infty$. When non-dimensionalized with respect to the ambient fluid with density $\rho_\infty$, speed of sound $c_\infty$, pressure $\rho_\infty c_\infty^2$, temperature $(\gamma - 1)T_\infty$ and the initial vorticity thickness $\delta_{\omega,0}$, the equation of state is written $p = [(\gamma - 1)/\gamma]\rho T$. The Reynolds number $Re = (\rho_\infty \Delta U \delta_{\omega,0}/\mu_\infty)$ is 500, with $\Delta U$ the velocity difference across the shear layer, and the Prandtl number is 0.71.

The calculation is carried out on a $704 \times 352$ grid on a domain of size $130\delta_{\omega,0} \times 65\delta_{\omega,0}$. The inflow forcing sponge region is noted in Fig. 8 and extends from the upstream computational boundary to one instability wavelength downstream. Additional details of the calculation, including the determination of the instability wave, are given in the appendix.

Denoting the instability wave solution as $q'$ and the time-averaged mean flow as $q_{\text{in}}$, the forcing sponge solution is chosen to be $q_{\text{ref}} = q_{\text{in}} + \epsilon q'$, with $0 < \epsilon \ll 1$, to introduce the instability waves into the shear layer. The inflow sponge region is taken to be one instability-wavelength long (see Fig. 8) and of the form

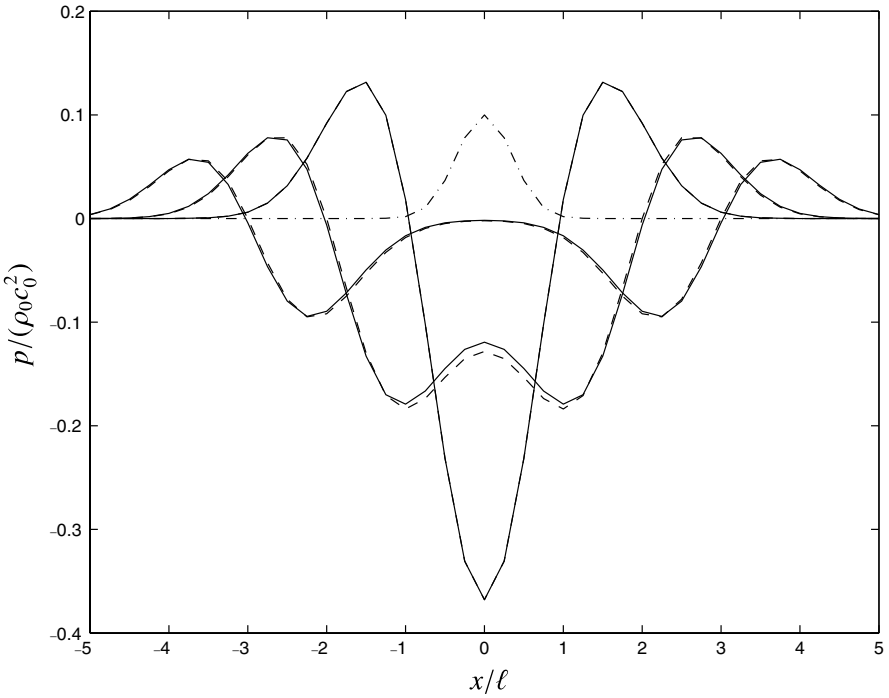


Fig. 7. Pressure field of the transient problem of a Gaussian sound pulse, centered at the origin, as initial data at $t = 0$ using the method of problem (3). Times $t = 1$, $t = 2$ and $t = 3$ are shown. Solid line ——, exact solution; dotted line – – –, numerical solution; dash-dot line –·–, penalty parameter $\sigma(x)/(10\sigma_{\max})$.

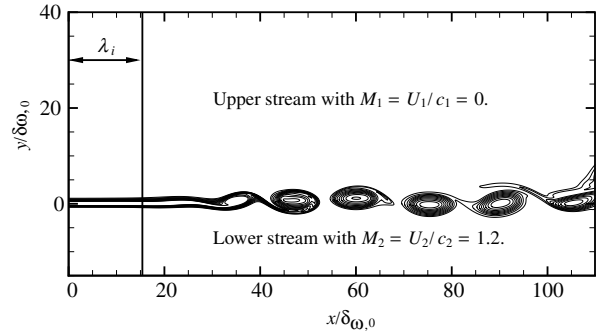


Fig. 8. Two-dimensional shear layer with vorticity contours.

$$\sigma = \begin{cases} A\left(\frac{\lambda_i - x}{\lambda_i}\right)^3 & \text{for } x < \lambda_i, \\ 0 & \text{otherwise,} \end{cases} \tag{63}$$

where $A$ is an adjustable parameter. Three values of $A$ were chosen: 0.1, 1.0 and 10.0.

For each value of $A$, the shear layer was forced and time-history data was collected along the shear layer centerline at $(x, y) = (\lambda_i, 0)\delta_{\omega,0}$, i.e., at the end of the sponge region. The pressure time traces at this location are shown in Fig. 9 along with the target instability-wave pressure. After an initial transient of $t = 20\delta_{\omega,0}/c_\infty$

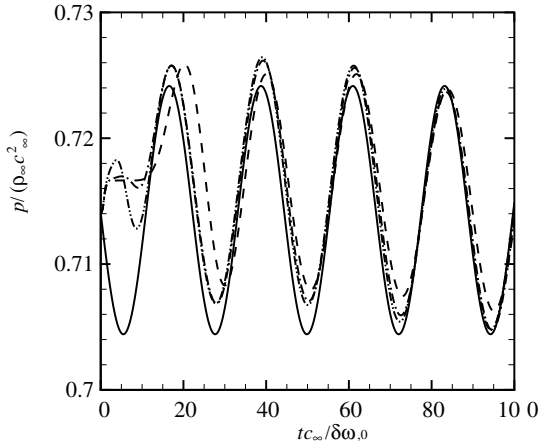


Fig. 9. Record pressure time histories taken at $(x,y) = (\lambda_i,0)\delta_{\omega,0}$. Legend: ——, $p$ using $A = 0.1$; –·–, $p$ using $A = 1.0$; $p$ using – · · –, $A = 10.0$; —, $p$ from the instability wave.

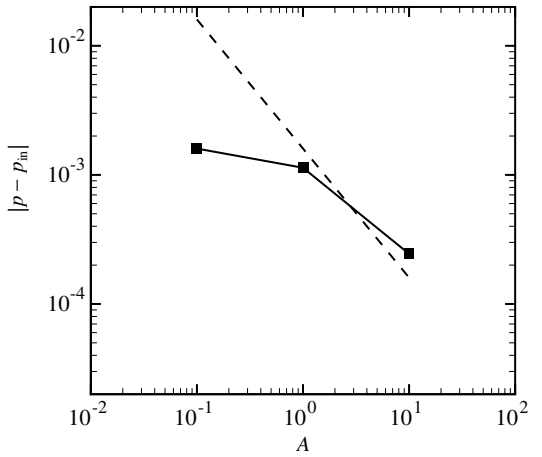


Fig. 10. Pressure difference at $(x,y) = (\lambda_i,0)\delta_{\omega,0}$ taken at $t = 100\delta_{\omega,0}/c_\infty$. Dashed line is proportional to $A^{-1}$.

the forced shear layer follows the general form of the desired wave form but with differences in the phase and amplitude depending on $A$. The weakest sponge with $A = 0.1$ differs the most from the target state; the strongest sponge differs the least. By $t = 80\delta_{\omega,0}/c_\infty$, the shear layer solution fairly well matches the target state. If one computes the difference between the computed and target state at $t = 100\delta_{\omega,0}/c_\infty$ as a function of $A$ (see Fig. 10) one finds (roughly) a $A^{-1}$ dependence for $A \geqslant 1$.

## 5. Practical guidelines

### 5.1. Functional shape of the penalty parameter

One lacking feature of the discussion so far is that there is no obvious method of picking $\sigma$: one, in practice, must specify both the shape and the maximum value of the penalty parameter. There have been a number of previously reported parameterizations of $\sigma$; see, for example, [6,8,14]. A brief summary of the results are

- One must choose $\sigma_{\max}$ sufficiently large to justify using the penalty method at all. When non-dimensionalized by the relevant time scale of the source, say $r = \sigma_{\max}/\omega_{\text{src}}$, practice has shown that values on the order of $10 < r < 100$ are sufficient to ensure the amplitude and phase of the original signal are captured in the extended field.
- There is an upper limit to $\sigma_{\max}$: for values of $\sigma_{\max}$ significantly large the numerical problem of becomes stiff and difficult to solve. This problem is also present in the original finite element computation of incompressible flow [16].
- It has been found that the overall extended, or forced, solution is somewhat robust to changes in $\sigma(x)/\sigma_{\max}$ for a given maximum value. That is, the smoothly diminishing exponential proposed in Eq. (61) may be replaced with a sharp 'top-hat' function

$$\sigma = \begin{cases} \sigma_{\max} & \text{for } r \leqslant r_0, \\ 0 & \text{otherwise} \end{cases}$$

without introducing unwanted behavior. This implies that one should take $\sigma$ to be a large, non-zero constant in the entire region where the original solution $u$ is known, thus permitting the domain on which $u$ is specified to be of arbitrary shape. This is in contrast to the results of Section 3 which found an *absorbing* sponge should be constructed to be smooth.

### 5.2. Influence of sponge zone on waveforms

There may be some residual effect of the shape of the domain $\Omega$ on the extended field $v$. To see this, consider a model problem in which the original field $u$ is an acoustic plane wave propagating in a quiescent medium. As this plane wave approaches the boundary $\partial\Omega$, it will intersect the boundary at different instances in time, depending on the wave direction and the shape of the boundary. In the case of plane waves approaching a straight boundary parallel to the wave fronts, the wave will intersect the boundary at the same time, but we do not consider this special case.

Along the direction of $k$, the wavenumber vector, the plane wave $u$ is one-dimensional so one may take the problem of finding the extended field $v$ to as being governed by the one-dimensional wave equation with position $x$ taken parallel to $k$. Then the equation for $v$ is

$$\frac{\partial^2 v}{\partial t^2} - \frac{\partial^2 v}{\partial x^2} = -\sigma\left(\frac{\partial v}{\partial t} - \frac{\partial u}{\partial t}\right) \tag{64}$$

for unity wave speed. Supposing that $u(x,t) = \exp(\mathrm{i}(k \cdot x - \omega\, t))$ one finds that $v$ has a component which decays like $\exp(-\sqrt{\sigma^2 - 1}k \cdot (x - x_B))$ for $x > x_B$. Due to the shape of the boundary $\partial\Omega$, the value of $x$ for which the plane wave intersects the boundary will be different, thus introducing some dependence of $\Omega$ on $v$.

To minimize this effect, the necessary steps are apparent. One may take $\sigma_{\max}$ to be as large as possible and/or increase the size of $\Omega$. Alternatively, if something is known about the shape of the waves traveling into $\Gamma$, then $\Omega$ may be shaped to minimize the anisotropy. For example, if spherical waves were produced in $\Omega$, choosing $\partial\Omega$ to be a sphere would be natural. In cases where the precise form of the forced solution is important, special care must be taken to minimize the imprint of the forcing sponge on the resultant solution.

### 5.3. Resonance

The analysis of Section 3 suggested that in cases where a long sponge zone exists with a constant penalty parameter, it is possible to create an unstable situation where the sponge acts as an unwanted source. Additionally, it appears that the inclusion of a damping sponge can remove a resonance condition only in special cases of the spatial form of $\sigma(x)$. To see this, consider a case that generalizes the reflection example of

Section 3.2. Instead of the one-sided reflection of Fig. 2 let there exist one-dimensional acoustic waves in the bounded region $-\mathscr{L} \leqslant x \leqslant \mathscr{L}$ generated by a source of frequency $\omega$. Additionally, let there exist two sponges of length $L < \mathscr{L}/2$ in the regions $-\mathscr{L} \leqslant x \leqslant -\mathscr{L} + L$ for the left sponge and $\mathscr{L} - L \leqslant x \leqslant \mathscr{L}$ for the right sponge. The sponge strength and shape are to be the same in both zones. For the hard-wall boundary conditions of $\hat{u}(-\mathscr{L}) = \hat{u}(\mathscr{L}) = 0$ the Green's function $\hat{u}_{\mathrm{G}}$ of (43), with $\hat{u}_{\mathrm{s}}$ replaced by $\hat{u}_{\mathrm{G}}$ and $\hat{s} = \delta(x - y)$, is given by (48) as

$$\hat{u}_{\mathrm{G}} = \begin{cases} A_{\mathrm{L}} y_1(-x - (\mathscr{L} - L)) + B_{\mathrm{L}} y_2(-x - (\mathscr{L} - L)) & \text{for } x < y, \\ A_{\mathrm{R}} y_1(x - (\mathscr{L} - L)) + B_{\mathrm{R}} y_2(x - (\mathscr{L} - L)) & \text{for } x > y, \end{cases} \tag{65}$$

where the constants $\{A_L, B_L, A_R, B_R\}$ are chosen to satisfy the boundary conditions at $x = \pm\mathscr{L}$ and the jump conditions at $x = y$. Integrating (43) and its first moment over the jump at $x = y$ shows that while $\hat{u}_{\mathrm{G}}$ is continuous at $x = y$ its first derivative satisfies the jump (see, for example, [23])

$$\left.\frac{\mathrm{d}\hat{u}_{\mathrm{G}}}{\mathrm{d}x}\right|_{y+} = \left.\frac{\mathrm{d}\hat{u}_{\mathrm{G}}}{\mathrm{d}x}\right|_{y-} + 1 \tag{66}$$

Utilizing the four conditions the four constants may be found. For the special case of a source localized near $x = 0$, the solution is

$$\hat{u}_{\mathrm{G}} = \begin{cases} \frac{C_{\mathrm{L}}}{\Delta} y_1(-x - (\mathscr{L} - L)) + \frac{D_{\mathrm{L}}}{\Delta} y_2(-x - (\mathscr{L} - L)) & \text{for } x < y \\ \frac{C_{\mathrm{R}}}{\Delta} y_1(x - (\mathscr{L} - L)) + \frac{D_{\mathrm{R}}}{\Delta} y_2(x - (\mathscr{L} - L)) & \text{for } x > y, \end{cases} \tag{67}$$

where $A_{\mathrm{R}} = C_{\mathrm{R}}/\Delta$, $B_{\mathrm{R}} = D_{\mathrm{R}}/\Delta$ and similarly for the left coefficients $A_{\mathrm{L}}$ and $B_{\mathrm{L}}$. The common denominator $\Delta$ takes the form, when $\sigma$ is given by (47) and appropriately scaled and reflected, of

$$\Delta = \begin{cases} 4\omega \sin\left(\frac{2\omega L}{c_0}\right) & \text{for } n \geqslant 0, \text{ even}, \\ 4\omega \cosh\left(\frac{\mathrm{i}\omega L}{c_0} + \frac{L\eta}{(n+1)c_0}\right) & \text{for } n > 0, \text{ odd}. \end{cases} \tag{68}$$

Thus when $n$ is even the sponge has no effect on the resonance properties of the system; that is, the sponge does not prevent resonance. In contrast, when $n$ is odd, the resonance is suppressed so long as $\eta > 0$; when $\eta \to 0$ the resonance returns at the same frequency as the undamped system.

Extrapolation of this analysis to more general systems is, of course, impossible but the results suggest that there may be conditions where sponge zones do not have the desired effect on system damping.

## 6. Conclusion

An analysis of sponge regions, which are commonly used to force a solution towards a target state, either unsteady or steady, at computational boundaries has shown that the rate of convergence between the actual and target states is proportional to $\|\sigma\|^{-1}$, where $\|\sigma\|$ is a measure of the sponge strength. When applied to the linearized equations of fluid mechanics, it was found that the sponge may unstably force the solution unless equal sponge strengths were used in each equation. In the case of one-dimensional acoustic wave propagation into a sponge strength of $\sigma = \eta(x/L)^n$, for positive integer $n$, the amplitude of the reflected wave scales as $\eta L \exp\{-\eta L/(n+1)\}$ for a sponge of length $L$. Numerical examples verify the $\|\sigma\|^{-1}$ convergence for linear, two-dimensional acoustic wave propagation. The efficacy of the forcing properties of the sponge is shown qualitatively for a transient acoustic pulse in three dimensions. In addition, the introduction of instability waves into a two-dimensional, compressible, viscous shear layer, governed by the full nonlinear equations, demonstrated a near $\|\sigma\|^{-1}$ convergence rate.

## Acknowledgments

The author thanks Prof. T.J.R. Hughes for his helpful discussions and constructive criticisms on this topic. This work was performed under financial support from the Department of Defense's National Defense Science and Engineering Graduate Fellowship, and in part by a grant from the Ohio Aerospace Institute. Additional support by the Center for Turbulence Research, Stanford, CA, is gratefully acknowledged.

## Appendix

Some details regarding the shear layer calculation are provided in this appendix. Consider the equations of motion for a two-dimensional compressible, viscous fluid for the conserved densities:

$$\begin{aligned}
&\frac{\partial \rho}{\partial t} + \frac{\partial \rho u_j}{\partial x_j} = -\sigma(\rho - \rho_{\mathrm{ref}}),\\
&\frac{\partial \rho u_i}{\partial t} + \frac{\partial}{\partial x_j}\left(\rho u_i u_j + p\delta_{ij} - \tau_{ji}\right) = -\sigma(\rho u_i - (\rho u_i)_{\mathrm{ref}}),\\
&\frac{\partial \rho E}{\partial t} + \frac{\partial}{\partial x_j}\left([\rho E + p]u_j + q_j - \tau_{ji}u_i\right) = -\sigma(\rho E - (\rho E)_{\mathrm{ref}}).
\end{aligned} \tag{69}$$

Here, the fluid has mass density $\rho$, momentum density $\rho u$, energy density $\rho E$ and pressure $p$. The viscous effects include the stress $\tau_{ij}$ and heat flux $q_j$. An ideal gas is assumed with the following constitutive relations:

$$\begin{aligned}
\tau_{ji} &= \mu(T)\left(\frac{\partial u_i}{\partial x_j} + \frac{\partial u_j}{\partial x_i}\right) + \lambda(T)\frac{\partial u_k}{\partial x_k}\delta_{ij},\\
q_j &= -k(T)\frac{\partial T}{\partial x_j},
\end{aligned} \tag{70}$$

where the temperature $T$ is given by $T = p/(R\rho)$ with specific gas constant $R$. The viscosity temperature dependence is tabulated by White [24] as $\mu/\mu_0 = (T/T_0)^n$ for $n = 2/3$. The second viscosity coefficient $\lambda$ is taken to be $\mu_{\mathrm{B}} + 2/3$ with $\mu_{\mathrm{B}}/\mu = 0.6$ [25].

At the inflow portion of the domain, near $x/\delta_{\omega,0} = 0$, the shear layer profile is governed by the similarity solution of the compressible boundary layer equations using the Howarth transformation [26]. If the inflow (at $x = 0\delta_{\omega,0}$) profile is denoted by $q_{\mathrm{in}}$ then the instability waves, or eigenfunctions, correspond to homogeneous solutions of the inviscid equations linearized about $q_{\mathrm{in}}$. Assuming the disturbance to be modal with a non-trivial $y$-structure $q' = \hat{q}(y)\exp\{\mathrm{i}(\omega t - \alpha x)\}$, with real frequency $\omega$ and complex eigenvalue $\alpha$, corresponding to the spatially developing disturbance, the vertical velocity $\hat{v}$ satisfies the compressible Rayleigh equation

$$\frac{\mathrm{d}^2\hat{v}}{\mathrm{d}y^2} - \frac{1}{\xi}\frac{\mathrm{d}\xi}{\mathrm{d}y}\frac{\mathrm{d}\hat{v}}{\mathrm{d}\,y} - \left(\frac{\alpha}{\omega - \alpha u_{\mathrm{in}}}\left[\frac{1}{\xi}\frac{\mathrm{d}u_{\mathrm{in}}}{\mathrm{d}y}\frac{\mathrm{d}\xi}{\mathrm{d}y} - \frac{\mathrm{d}^2 u_{\mathrm{in}}}{\mathrm{d}y^2}\right] - \rho_{\mathrm{in}}\xi\right)\hat{v} = 0, \tag{71}$$

with $\xi = (\omega - \alpha u_{\mathrm{in}})^2 - c_{\mathrm{in}}^2\alpha^2$. We seek solutions to (71) corresponding to the Kelvin–Helmoltz (discrete) modes that satisfy the boundary conditions $\hat{v} \sim \exp\{-\sqrt{\rho_{\mathrm{in}}\xi}\|y\|\}$ as $\|y\| \to \infty$.

Solution of the eigenvalue problem (71) is accomplished using a shooting technique to determine $\alpha$ from a given real-valued $\omega$. With the $(\omega, \alpha)$ pair determined Rayleigh's equation (71) is integrated to determine the disturbance mode shape $\hat{v}$. The disturbance profiles of the conservative variables are found by linear combinations of $\hat{v}$ and its $y$-derivative. For a frequency of $\omega = 0.2831c_\infty/\delta_{\omega,0}$ the eigenvalue $\alpha$ is $(0.4086 - 0.1994\mathrm{i})\delta_{\omega,0}^{-1}$ which corresponds to a downstream-traveling instability wave with $x$-direction wavelength of $\lambda_i = 2\pi/\alpha_r = 15.4\delta_{\omega,0}$ and a phase speed of $\omega/\alpha_r = 0.7a_\infty$.

## References

[1] J.B. Freund, Noise sources in a low-Reynolds-number turbulent jet at Mach 0.9, J. Fluid Mech. 438 (2001) 277–305.
[2] W. Zhao, S.H. Frankel, L. Mongeau, Large eddy simulations of sound radiation from subsonic turbulent jets, AIAA J. 39 (8) (2001) 1469–1477.
[3] C. Lui, S.K. Lele, Sound generation mechanism of shock-associated Noise, AIAA Paper 2003-3315, Presented at the 9th AIAA/CEAS Aeroacoustics Conference, Hilton Head Island, South Carolina, 2003.
[4] D.J. Bodony, S.K. Lele, On using large-eddy simulation of the prediction of noise from cold and heated turbulent jets, Phys. Fluids 17 (2005) 085103.
[5] J.U. Schlüter, H. Pitsch, P. Moin, Consistent boundary conditions for integrated les/rans simulations: Les outflow conditions, AIAA Paper 2002-3121, Presented at the 32nd AIAA Fluid Dynamics Conference and Exhibit, St. Louis, MO, 24–27 June, 2002.
[6] M. Israeli, S.A. Orszag, Approximation of radiation boundary conditions, J. Comp. Phys. 41 (1981) 115–135.
[7] J. Nordström, N. Nordin, D. Henningson, The fringe region technique and the Fourier method used in the direct numerical simulation of spatially evolving viscous flows, SIAM J. Sci. Comput. 20 (4) (1999) 1365–1393.
[8] J.B. Freund, A simple method for computing far-field sound in aeroacoustic computations, J. Comp. Phys. 157 (2000) 796–800.
[9] J.-P. Berenger, A perfectly matched layer for the absorption of electromagnetic waves, J. Comp. Phys. 114 (1994) 185–200.
[10] F.Q. Hu, On absorbing boundary conditions for linear Euler equations by a perfectly matched layer, J. Comp. Phys. 129 (1996) 201–219.
[11] F.Q. Hu, On using perfectly matched layer for the euler equations with a non-uniform mean flow, AIAA Paper 2004–2966, Presented at the 10th AIAA/CEAS Aeroacoustics Conference and Exhibit, Manchester, UK, 10–12 May, 2004.
[12] J.S. Hesthaven, On the analysis and construction of perfectly matched layers for the linearized euler equations, J. Comp. Phys. 142 (1998) 129–147.
[13] T. Colonius, H. Ran, A super-grid-scale model for simulating compressible flow on unbounded domains, J. Comp. Phys. 182 (2002) 191–212.
[14] T. Colonius, Modeling artificial boundary conditions for compressible flow, Ann. Rev. Fluid Mech. 36 (2004) 315–345.
[15] R. Temam, Navier–Stokes Equations: Theory and Approximation, North-Holland, Amsterdam, 1977.
[16] T.J.R. Hughes, W.K. Liu, A. Brooks, Finite element analysis of incompressible viscous flows by the penalty function formulation, J. Comp. Phys. 30 (1979) 1–60.
[17] L.C. Evans, Partial Differential Equations, American Mathematical Society, Providence, RI, 1998.
[18] F. Brezzi, M. Fortin, Mixed and Hybrid Finite Element Methods, Springer, New York, NY, 1991.
[19] E.A. Coddington, N. Levinson, Theory of Ordinary Differential Equations, McGraw-Hill Book Company, Inc., New York, USA, 1955.
[20] J.D. Cole, On a quasi-linear parabolic equation occuring in aerodynamics, Quart. Appl. Math. 9 (1951) 225–236.
[21] T.J. Poinsot, S.K. Lele, Boundary conditions for direct simulations of compressible viscous flows, J. Comp. Phys. 101 (1992) 104–129.
[22] G.S. Constantinescu, S.K. Lele, Large Eddy Simulation Of a Nearly Sonic Turbulent Jet and Its Radiated Noise, AIAA Paper 2001–0376, Presented at the 39th Aerospace Sciences Meeting and Exhibit, Reno, NV, 2001.
[23] C.M. Bender, S.A. Orszag, Advanced Mathematical Methods for Scientists and Engineers, Springer, New York, NY, 1999.
[24] F.M. White, Viscous Fluid Flow, second ed., McGraw-Hill, Inc., USA, 1991.
[25] P.A. Thompson, Compressible-Fluid Dynamics, McGraw-Hill, New York, 1988.
[26] H. Schlichting, Boundary-Layer Theory, fourth ed., McGraw-Hill, New York, NY, 1979.